

RESEARCH

Open Access



Rich dynamics of a Filippov avian-only influenza model with a nonsmooth separation line

Youping Yang^{1*} and Jingwen Wang¹

*Correspondence:

yyang@sdu.edu.cn

¹School of Mathematics and Statistics, Shandong Normal University, 250014, Jinan, China

Abstract

Depopulation of birds has been authenticated to be an effective measure in controlling avian influenza transmission. In this work, we establish a Filippov avian-only model incorporating a threshold policy control. We choose the index—the maximum between the infected threshold level I_T and the product of the number of susceptible birds S and a ratio threshold value ξ —to decide on whether to trigger the control measures or not, which then leads to a discontinuous separation line and two pieces of sliding-mode domains. Meanwhile, one more sliding-mode domain gives birth to more complex dynamics. We investigate the global dynamical behavior of the Filippov model, including the real and/or virtual equilibria and the two sliding modes and their dynamics. The solutions will eventually stabilize at the real endemic equilibrium of the subsystem or the pseudoequilibria on the two sliding modes due to different threshold values. Therefore an effective and efficient threshold policy is essential to control the influenza by driving the number of infected birds below a certain level or at a previously given level.

Keywords: Nonsmooth threshold policy; Filippov control; Global stability; Sliding modes

1 Introduction

Highly pathogenic avian influenza A virus causes high flock mortality [1]. The disease not only causes significant social and economic loss on domestic fowl in affected areas [2] but composes a potentially serious threat for humans [3, 4]. Governments worldwide have paid a lot to treat the patients and control the pandemic [5]. Hence, it is an emergent issue to identify any effective control strategies to eliminate the influenza or at least to reduce the impact to a tolerant level; in particular, bringing down the number of infected birds becomes a priority.

The Chinese government has begun to release avian influenza A(H7N9) data via websites and official news agency daily since the first case was reported in March 2013 [6]. Hence people could understand the progress and then avoid some unnecessary contact. At the same time, some cities like Nanjing, Guangzhou, and Shanghai have closed sev-

© The Author(s) 2021. This article is licensed under a Creative Commons Attribution 4.0 International License, which permits use, sharing, adaptation, distribution and reproduction in any medium or format, as long as you give appropriate credit to the original author(s) and the source, provide a link to the Creative Commons licence, and indicate if changes were made. The images or other third party material in this article are included in the article's Creative Commons licence, unless indicated otherwise in a credit line to the material. If material is not included in the article's Creative Commons licence and your intended use is not permitted by statutory regulation or exceeds the permitted use, you will need to obtain permission directly from the copyright holder. To view a copy of this licence, visit <http://creativecommons.org/licenses/by/4.0/>.

eral poultry markets, culled poultry and disinfected the environment, and the first two measures were proved to be more effective in controlling A(H7N9) infections [7].

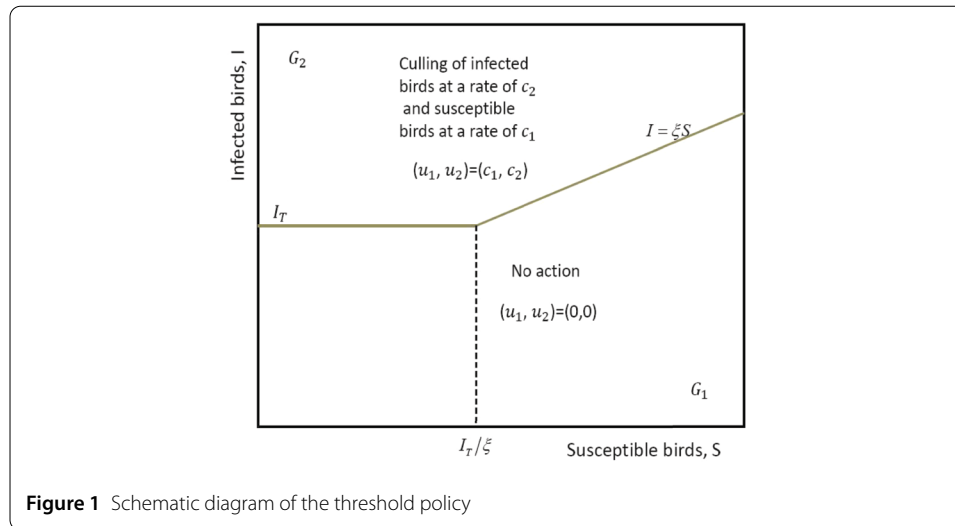
Indeed, depopulation of infected birds and those with close contact has been authenticated to be an effective measure in controlling avian influenza transmission, however, this is also a risky enterprise with the risk of killing the susceptible birds during the infection prevention [8, 9]. Therefore the identified culling strategy should not only be effective but also efficient to avoid overkilling of the susceptible birds, and then further establish a balance among acceptable control measures safeguarding the livelihoods of farmers and the health of the population [10].

Mathematical modeling is a useful tool and has been applied widely to illustrate the transmission dynamics of various pandemic diseases. Based on the epidemiology and different control strategies, ordinary differential equations [11, 12], delay differential equations [13–16], and discrete differential equations [17] have been proposed and analyzed. Andronico et al. [18] established a mathematical model to study the spatiotemporal evolution of the disease and evaluate the impact of control measures. The authors obtained that a faster culling of diagnosed infected targets would have a larger impact on the total number of infections.

Several conventional control methods considering a threshold policy may be employed in disease management. A threshold policy is such that there exists a tolerance threshold so that whenever the number of the infected is below that threshold, the infection is considered to be tolerable. Otherwise, the infection might cause intolerable economic damage. Mathematical models with a threshold policy, which is biologically and economically desirable, are described by the so-called Filippov systems with discontinuous right-hand sides [19–21].

Xiao et al. [22] extended the classical SIR model to a Filippov SIR model by including a piecewise incidence rate to represent behavioral change of general individuals and implementation of necessary precautionary measures. They suggested that choosing a proper combination of threshold and control intensities based on a threshold policy can preclude outbreaks or stabilize the infection at a desired level. Zhou et al. [23] proposed a Filippov-type model of interrupting transmission of West Nile virus to birds by implementing culling of mosquitoes once the number of infected birds exceeds a threshold level. They showed that strengthening the culling of mosquitoes together with protecting birds is a good choice in controlling the spread of West Nile virus. Bolzoni et al. [24] studied a two-patches metapopulation mathematical model in wildlife diseases. They considered both proactive and reactive localized culling strategies. The localized reactive control is described by a Filippov system with a piecewise-constant culling effort function. The authors indicated that when the host fecundity is affected by the infection, localized culling may be ineffective in controlling wildlife diseases.

Chong et al. [25] considered an avian-only model considering a threshold policy. The authors chose the number of infected birds as an index, that is, once the index exceeds the threshold level I_T , culling of infected birds is employed, otherwise, no action is taken. However, when the number of infected birds exceeds the threshold level I_T and the number of susceptible birds is large enough, it is not always necessary to take control strategies. In fact, if the interaction ratio of the number of infected and susceptible birds is smaller than a ratio threshold value, then more effort is needed to take care of the susceptible birds to maximize the profits rather than to take control strategies, which then could lead to la-



bor shortage and cause economic loss for farmers. This nonsmooth threshold mechanism has been adopted by Li et al. [26] for a plant disease model. Therefore, reconsidering the avian-only model in [25] by incorporating this kind of a threshold policy may be more reasonable, which also results in a nonsmooth separation line compared to the model in [25].

The rest of the paper is structured as follows. In Sect. 2, we establish an avian-only Filippov model with considering a more realistic threshold policy which leads to a nonsmooth separation line. The dynamical behavior of the proposed Filippov system, including the real and/or virtual equilibria, the two sliding-mode domains and their dynamics is investigated in Sects. 3–5. We conclude this work in Sect. 6.

2 Filippov avian-only model

In order to better control the avian influenza transmission, minimize the economic damage, and optimize the profits, control strategies should be applied based on whether the number of infected birds and/or the interaction ratio of the number of infected and susceptible birds exceed the given tolerant threshold levels or not. If the number of infected birds is below the infected threshold level I_T , then no control is taken; above I_T , the control strategies should be carried out depending on the number of susceptible birds and the interaction ratio of the number of infected and susceptible birds. When the number of susceptible birds S is small ($S < \frac{I_T}{\xi}$), we cull infected birds at a rate of c_2 and susceptible birds at a rate of c_1 , $c_i > 0, i = 1, 2$, respectively. Whilst when the number of susceptible birds is large enough ($S > \frac{I_T}{\xi}$) and the interaction ratio is below the ratio threshold value ξ , which means the number of infected birds is relatively small compared to the susceptible birds, then the control strategy is not taken to save the effort and maximize the profits; otherwise, if the interaction ratio exceeds the ratio threshold value ξ , control measures are triggered. A schematic diagram depicting the threshold policy is shown in Fig. 1. The reason for culling susceptible birds is that as the influenza progresses, more susceptible birds may be infected later and cause a more severe outbreak, here we assume $c_1 < c_2$.

Chong et al. [25] assumed that the avian populations are subject to the rule of constant growth. But migrant birds are mostly viewed as the original infection source [12, 27]. Pathogens may be transmitted to new areas by migratory hosts, which leads to new host

species' exposure and potential infection. Then those resident hosts, which are immunologically naive to these novel pathogens, may subsequently act as local amplifiers [18]. For example, West Nile virus's global spread is greatly facilitated by migratory birds, which transmit the pathogens to other wildlife and humans in many parts of the world [28]. It is well known that the logistic growth is more reasonable than the constant growth for the wildlife birds, including resident and migratory birds [12]. Hence, we choose logistic growth here for avian populations. Let $S(t)$ and $I(t)$ denote the numbers of susceptible and infected birds at time t . The susceptible birds are subject to logistic growth $rS(1 - S/K)$, where r is the intrinsic growth rate and K is the maximal carrying capacity.

Then the Filippov avian-only model with a nonsmooth separation line can be listed by the following system:

$$\begin{pmatrix} S' \\ I' \end{pmatrix} = \begin{pmatrix} rS(1 - \frac{S}{K}) - \beta SI - u_1 S \\ \beta SI - \mu I - dI - u_2 I \end{pmatrix} = \begin{pmatrix} f_1(S, I) \\ f_2(S, I) \end{pmatrix}, \tag{1}$$

with

$$(u_1, u_2) = \begin{cases} (0, 0) & \text{for } I - \max\{I_T, \xi S\} < 0, \\ (c_1, c_2) & \text{for } I - \max\{I_T, \xi S\} > 0, \end{cases} \tag{2}$$

where β is the transmission rate of the disease from infected birds I to susceptible birds S , μ is the natural death rate, d is the disease-induced death rate. Here we assume $r > c_1$ and $\xi > 0$; when $\xi = 0$, it becomes the model in [25] with constant growth.

Denote the nonsmooth separation line as $\Omega = \{(S, I) \in R_+^2 : H(S, I) = I - \max\{I_T, \xi S\} = 0\}$, then the S, I space R_+^2 consists of the following four regions:

$$\begin{aligned} G_1 &= \{(S, I) \in R_+^2 : I < \max\{I_T, \xi S\}\}, \\ G_2 &= \{(S, I) \in R_+^2 : I > \max\{I_T, \xi S\}\}, \\ \Omega_1 &= \{(S, I) \in R_+^2 : I = I_T, S < I_T/\xi\}, \\ \Omega_2 &= \{(S, I) \in R_+^2 : I = \xi S, S > I_T/\xi\}. \end{aligned}$$

The dynamics in subregion G_i are governed by $F_i, i = 1, 2$, where

$$F_1(S, I) = \begin{pmatrix} F_{11}(S, I) \\ F_{12}(S, I) \end{pmatrix} = \begin{pmatrix} rS(1 - \frac{S}{K}) - \beta SI \\ \beta SI - \mu I - dI \end{pmatrix}, \tag{3}$$

$$F_2(S, I) = \begin{pmatrix} F_{21}(S, I) \\ F_{22}(S, I) \end{pmatrix} = \begin{pmatrix} rS(1 - \frac{S}{K}) - \beta SI - c_1 S \\ \beta SI - \mu I - dI - c_2 I \end{pmatrix}. \tag{4}$$

Note that the manifolds Ω_1 and Ω_2 are discontinuity surfaces connecting the two different structures of system (1)–(2). We consider the solutions of system (1)–(2) in Filippov's sense, as the right-hand side of the system is discontinuous. The theory of existence and uniqueness of solutions of Filippov systems is developed and can be found in [29]. We present the definitions of real equilibrium, virtual equilibrium, sliding mode, and pseudo-equilibrium that are necessary throughout the paper [26, 30–33].

Definition 2.1 E^R is called a real equilibrium of system (1)–(2) if $F_1(E^R) = 0, E^R \in G_1$ or $F_2(E^R) = 0, E^R \in G_2$; E^V is called a virtual equilibrium of system (1)–(2) if $F_1(E^V) = 0, E^V \in G_2$ or $F_2(E^V) = 0, E^V \in G_1$.

Definition 2.2 If there exists a subset Σ of the manifold Ω_i such that the flows of f (outside of Ω_i) are directed towards each other on them, $i = 1, 2$, then Σ is called a sliding mode.

By applying the well-known Filippov convexity method [29] or Utkin’s equivalent control method [34], we can obtain the dynamics on the sliding mode. Here we present the Filippov convexity method, that is,

$$\frac{dx}{dt} = \sigma F_1 + (1 - \sigma)F_2 = \Psi(S, I), \quad x = (S, I)^T \in \Sigma,$$

where $\sigma = \frac{\langle \nabla H, F_2 \rangle}{\langle \nabla H, F_2 - F_1 \rangle}$, $(\cdot)^T$ means the transpose of the vector, $\langle \cdot, \cdot \rangle$ denotes the standard scalar product.

Definition 2.3 E^P is called a pseudoequilibrium if E^P is an equilibrium on the sliding mode Σ , that is, $\Psi(E^P) = 0$ and $E^P \in \Sigma \subset \Omega_i, i = 1, 2$.

2.1 Dynamics in subregion $G_i, i = 1, 2$

By applying the next generation matrix method [35], we can obtain the basic reproduction number R_{0i} for the system in region $G_i, i = 1, 2$,

$$R_{01} = \frac{K\beta}{\mu + d}, \quad R_{02} = \frac{K\beta(1 - \frac{c_1}{r})}{\mu + d + c_2}.$$

The equilibria of the system in region G_i are two disease-free equilibria, E_{i0}^1 and E_{i0}^2 , and a unique endemic equilibrium $E_i = (S_i^*, I_i^*)$ if $R_{0i} > 1, i = 1, 2$, where

$$\begin{aligned} E_{10}^1 &= (0, 0), & E_{10}^2 &= (K, 0), & E_1 &= (S_1^*, I_1^*) = \left(\frac{\mu + d}{\beta}, \frac{1}{\beta} \left(r - \frac{r(\mu + d)}{K\beta} \right) \right), \\ E_{20}^1 &= (0, 0), & E_{20}^2 &= \left(K \left(1 - \frac{c_1}{r} \right), 0 \right), \\ E_2 &= (S_2^*, I_2^*) = \left(\frac{\mu + d + c_2}{\beta}, \frac{1}{\beta} \left(r - c_1 - \frac{r(\mu + d + c_2)}{K\beta} \right) \right). \end{aligned}$$

The system in subregions G_1 and G_2 has been studied with different methods, here we just present the main results; more detailed proofs can be found in [9, 12].

Proposition 2.1 (i) The disease-free equilibrium E_{i0}^1 of the system in subregion G_i is always unstable; (ii) If $R_{0i} \leq 1$, the disease-free equilibrium E_{i0}^2 of the system in subregion G_i is globally asymptotically stable; (iii) If $R_{0i} > 1$, the endemic equilibrium E_i of the system in subregion G_i is globally asymptotically stable, $i = 1, 2$.

In the following three sections (Sects. 3–5), we investigate the existence and global stability of the real equilibrium, virtual equilibrium, and the pseudoequilibria on the two sliding modes with different threshold values. By Proposition 2.1, we only consider the case

when $R_{0i} > 1$, then system F_i in each subregion G_i admits the unique global asymptotical stable endemic equilibrium $E_i, i = 1, 2$. Since $S_1^* < S_2^*$, we then consider the following three cases generated by $S_1^* < S_2^* < \frac{I_T}{\xi}, S_1^* < \frac{I_T}{\xi} < S_2^*$, and $\frac{I_T}{\xi} < S_1^* < S_2^*$. We illustrate the dynamical behaviors of system (1)–(2) from one case to another.

3 Case A: global dynamics when $S_1^* < S_2^* < \frac{I_T}{\xi} (\xi < \frac{I_T}{S_2^*})$

3.1 Sliding mode on Ω_1 and its dynamics

Firstly, we present the existence of the sliding mode and its dynamics on the discontinuity surface Ω_1 . Since the scalar function $H(S, I) = I - I_T$ on $\Omega_1, \nabla H = (0, 1)^T$, then it can be easily obtained that

$$\langle \nabla H, F_1 \rangle|_{x \in \Omega_1} = \beta I_T (S - S_1^*), \quad \langle \nabla H, F_2 \rangle|_{x \in \Omega_1} = \beta I_T (S - S_2^*).$$

For $S_1^* < S_2^* < \frac{I_T}{\xi}$, therefore, by Definition 2.2 of the sliding mode, we can obtain the sliding-mode domain $\Sigma_1 \subset \Omega_1$ as follows:

$$\Sigma_1 = \{(S, I) \in \Omega_1 : S_1^* < S < S_2^*\}. \tag{5}$$

Here, we apply the Filippov convexity method [36, 37] to obtain the sliding-mode dynamics along the sliding mode Σ_1 ,

$$\begin{pmatrix} S' \\ I' \end{pmatrix} = \sigma_1 F_1 + (1 - \sigma_1) F_2, \quad \text{where } \sigma_1 = \frac{\langle \nabla H, F_2 \rangle}{\langle \nabla H, F_2 - F_1 \rangle}.$$

That is,

$$\begin{cases} S' = rS(1 - \frac{S}{K}) - \beta SI_T - \frac{c_1}{c_2} S(\beta S - \mu - d), \\ I' = 0. \end{cases} \tag{6}$$

System (6) has a unique positive equilibrium, denoted by $E_{p1} = (S_{p1}^*, I_T)$, where

$$S_{p1}^* = \frac{r - \beta I_T + \frac{c_1}{c_2}(\mu + d)}{\frac{r}{K} + \frac{c_1}{c_2}\beta},$$

if $I_T < \frac{r + \frac{c_1}{c_2}(\mu + d)}{\beta} = g_1$.

Next, we present the conditions for E_{p1} to be a pseudoequilibrium on $\Sigma_1 \subset \Omega_1$ and investigate its stability.

Proposition 3.1 E_{p1} is a pseudoequilibrium on $\Sigma_1 \subset \Omega_1$ if and only if $S_1^* < S_{p1}^* < S_2^*$, that is, $I_2^* < I_T < I_1^*$.

Theorem 3.1 E_{p1} is stable on $\Sigma_1 \subset \Omega_1$ when it is a pseudoequilibrium.

Proof It can be obtained by simple calculation that

$$\frac{\partial}{\partial S} \left(rS \left(1 - \frac{S}{K} \right) - \beta SI_T - \frac{c_1}{c_2} S(\beta S - \mu - d) \right) \Big|_{E_{p1}} = -\frac{r}{K} S_{p1}^* - \frac{c_1}{c_2} \beta S_{p1}^* < 0.$$

Hence, E_{p1} is stable. □

3.2 Sliding mode on Ω_2 and its dynamics

Since the scalar function $H(S, I) = I - \xi S$ on Ω_2 , $\nabla H = (-\xi, 1)^T$, then we can obtain that

$$\begin{aligned} \langle \nabla H, F_1 \rangle|_{x \in \Omega_2} &= \xi S \left(\frac{r}{K} + \xi \beta + \beta \right) (S - S^-), \\ \langle \nabla H, F_2 \rangle|_{x \in \Omega_2} &= \xi S \left(\frac{r}{K} + \xi \beta + \beta \right) (S - S^+), \end{aligned}$$

where

$$S^- = \frac{r + \mu + d}{\frac{r}{K} + \xi \beta + \beta}, \quad S^+ = \frac{r + \mu + d + c_2 - c_1}{\frac{r}{K} + \xi \beta + \beta}.$$

Denote

$$\begin{aligned} H_1 &= \frac{I_T \left(\frac{r}{K} + \frac{c_1}{c_2} \beta \right)}{r + \frac{c_1}{c_2} (\mu + d) - \beta I_T}, \\ H_2 &= \frac{I_T \left(\frac{r}{K} + \beta \right)}{r + \mu + d - \beta I_T}, \\ H_3 &= \frac{I_T \left(\frac{r}{K} + \beta \right)}{r + \mu + d + c_2 - c_1 - \beta I_T}, \\ g_1 &= \frac{r + \frac{c_1}{c_2} (\mu + d)}{\beta}, \quad g_2 = \frac{r + \mu + d}{\beta}, \quad g_3 = \frac{r + \mu + d + c_2 - c_1}{\beta}. \end{aligned}$$

Obviously, we have $H_2 > H_3$, $g_1 < g_2 < g_3$.

Proposition 3.2 *According to different values of I_T and ξ , we have the following results:*

(i) *If $I_T < g_2$ and $\xi > H_2$, then $\frac{I_T}{\xi} < S^-$ and the sliding-mode domain on Ω_2 is*

$$\Sigma_2 = \{(S, I) \in \Omega_2 : S^- < S < S^+\};$$

(ii) *If $I_T < g_2$ and $H_3 < \xi < H_2$ or $g_2 < I_T < g_3$ and $\xi > H_3$, then $S^- < \frac{I_T}{\xi} < S^+$ and the sliding-mode domain on Ω_2 is*

$$\Sigma_2 = \left\{ (S, I) \in \Omega_2 : \frac{I_T}{\xi} < S < S^+ \right\};$$

(iii) *If $I_T > g_3$ or $I_T < g_3$ and $\xi < H_3$, then $S^+ < \frac{I_T}{\xi}$ and there does not exist a sliding-mode domain on Ω_2 .*

Again, we apply the Filippov convexity method [36, 37] to obtain the sliding-mode dynamics along the sliding mode Σ_2 ,

$$\begin{pmatrix} S' \\ I' \end{pmatrix} = \sigma_2 F_1 + (1 - \sigma_2) F_2 \quad \text{where } \sigma_2 = \frac{\langle \nabla H, F_2 \rangle}{\langle \nabla H, F_2 - F_1 \rangle}.$$

That is,

$$\begin{cases} S' = \frac{S}{c_2 - c_1} \{rc_2(1 - \frac{S}{K}) - c_2\xi\beta S - c_1(\beta S - \mu - d)\} = g(S), \\ I' = \xi g(S). \end{cases} \tag{7}$$

System (7) admits a unique positive equilibrium $E_{p2} = (S_{p2}^*, \xi S_{p2}^*)$, where

$$S_{p2}^* = \frac{r + \frac{c_1}{c_2}(\mu + d)}{\frac{r}{K} + \xi\beta + \frac{c_1}{c_2}\beta}.$$

Theorem 3.2 E_{p2} is stable on $\Sigma_2 \subset \Omega_2$ when it is a pseudoequilibrium.

Proof We have

$$\frac{\partial g(S)}{\partial S} \Big|_{E_{p2}} = \frac{S_{p2}^*}{c_1 - c_2} \left(\frac{r}{K} c_2 + c_2 \xi \beta + c_1 \beta \right) < 0,$$

since $c_1 < c_2$. Hence, E_{p2} is stable. □

The following result gives the conditions for E_{p2} to be a pseudoequilibrium on $\Sigma_2 \subset \Omega_2$.

Proposition 3.3 According to the relationship between S^-, S^+ , and $\frac{I_T}{\xi}$, we have:

- (i) If $\frac{I_T}{\xi} < S^-$, that is, $I_T < g_2$ and $\xi > H_2$, E_{p2} becomes a pseudoequilibrium on $\Sigma_2 \subset \Omega_2$ if and only if

$$\frac{I_2^*}{S_2^*} < \xi < \frac{I_1^*}{S_1^*};$$

- (ii) If $S^- < \frac{I_T}{\xi} < S^+$, that is, $I_T < g_2$ and $H_3 < \xi < H_2$ or $g_2 < I_T < g_3$ and $\xi > H_3$, E_{p2} becomes a pseudoequilibrium on $\Sigma_2 \subset \Omega_2$ if and only if

$$I_T < g_1 \quad \text{and} \quad \xi > \max \left\{ \frac{I_2^*}{S_2^*}, H_1 \right\}.$$

Proof (i) If $\frac{I_T}{\xi} < S^-$, then E_{p2} becomes a pseudoequilibrium on $\Sigma_2 \subset \Omega_2$ if and only if $S^- < S_{p2}^* < S^+$. On the other hand, we have

$$\begin{aligned} S^- < S_{p2}^* &\iff \frac{r + \mu + d}{\frac{r}{K} + \xi\beta + \beta} < \frac{r + \frac{c_1}{c_2}(\mu + d)}{\frac{r}{K} + \xi\beta + \frac{c_1}{c_2}\beta} \\ &\iff (r + \mu + d) \left(c_2 \frac{r}{K} + c_2 \xi \beta + c_1 \beta \right) < (c_2 r + c_1(\mu + d)) \left(\frac{r}{K} + \xi \beta + \beta \right) \\ &\iff \xi < \frac{r}{\mu + d} - \frac{r}{K\beta} = \frac{\beta}{\mu + d} \cdot \frac{1}{\beta} \left[r - \frac{r(\mu + d)}{K\beta} \right] = \frac{I_1^*}{S_1^*}. \end{aligned}$$

Similarly, $S_{p2}^* < S^+ \iff \xi > \frac{I_2^*}{S_2^*}$. Hence, the result is obtained.

(ii) If $S^- < \frac{I_T}{\xi} < S^+$, then E_{p2} becomes a pseudoequilibrium on $\Sigma_2 \subset \Omega_2$ if and only if $\frac{I_T}{\xi} < S_{p2}^* < S^+$. And

$$\begin{aligned} \frac{I_T}{\xi} < S_{p2}^* &\iff \xi(c_2r + c_1(\mu + d)) > c_2I_T \frac{r}{K} + c_2\beta I_T \xi + c_1\beta I_T \\ &\iff \xi(c_2r + c_1(\mu + d) - c_2\beta I_T) > c_2I_T \frac{r}{K} + c_1\beta I_T \\ &\iff \xi > H_1, I_T < g_1. \end{aligned}$$

Together with $S_{p2}^* < S^+$, that is, $\xi > \frac{I_2^*}{S_2^*}$, one can obtain the result. □

The next proposition will play a crucial role in the following analysis.

Proposition 3.4 *We have:*

- $I_T < I_2^*$ if and only if $H_1 < H_3 < H_2, H_1 < \frac{I_2^*}{S_2^*}, H_3 < \frac{I_2^*}{S_2^*}, \frac{I_T}{S_2^*} > H_1, \frac{I_T}{S_2^*} > H_3, \frac{I_T}{S_2^*} < \frac{I_2^*}{S_2^*}$;
- $I_2^* < I_T < I_1^*$ if and only if $H_3 < H_1 < H_2$;
- $I_T > I_1^*$ if and only if $H_3 < H_2 < H_1, H_1 > \frac{I_1^*}{S_1^*}, H_2 > \frac{I_1^*}{S_1^*}, \frac{I_T}{S_1^*} < H_1, \frac{I_T}{S_1^*} < H_2, \frac{I_T}{S_1^*} > \frac{I_1^*}{S_1^*}$.

Proof Here we present the proof for $I_T < I_2^* \iff H_1 < \frac{I_2^*}{S_2^*}$, the other results can be obtained by applying the same method. There holds

$$\begin{aligned} H_1 < \frac{I_2^*}{S_2^*} &\iff \frac{I_T(\frac{r}{K} + \frac{c_1}{c_2}\beta)}{r + \frac{c_1}{c_2}(\mu + d) - \beta I_T} < \frac{\beta}{\mu + d + c_2} \frac{1}{\beta} \left(r - c_1 - \frac{r(\mu + d + c_2)}{K\beta} \right) \\ &\iff I_T \left(\frac{r}{K} + \frac{c_1}{c_2}\beta \right) (\mu + d + c_2) < \left(r + \frac{c_1}{c_2}(\mu + d) - \beta I_T \right) \left(r - c_1 - \frac{r(\mu + d + c_2)}{K\beta} \right) \\ &\iff \beta I_T \left(r + \frac{c_1}{c_2}(\mu + d) \right) < \left(r + \frac{c_1}{c_2}(\mu + d) \right) \left(r - c_1 - \frac{r(\mu + d + c_2)}{K\beta} \right) \\ &\iff I_T < \frac{1}{\beta} \left(r - c_1 - \frac{r(\mu + d + c_2)}{K\beta} \right) = I_2^*. \end{aligned}$$

Hence, the result is obtained. □

We present the relationships between the seven variables $\frac{I_i^*}{S_i^*}, \frac{I_T}{S_i^*}, H_j, i = 1, 2, j = 1, 2, 3$ related to I_1^*, I_2^* , and I_T , which play a vital role throughout the following analysis.

Proposition 3.5 *We have:*

(i) *If $I_T < I_2^* < I_1^*$, then*

$$H_1 < H_3 < H_2 < \frac{I_T}{S_1^*} < \frac{I_1^*}{S_1^*}, \quad H_3 < \frac{I_T}{S_2^*} < \frac{I_T}{S_1^*}, \quad \frac{I_T}{S_2^*} < \frac{I_2^*}{S_2^*} < \frac{I_1^*}{S_1^*};$$

(ii) *If $I_2^* < I_T < I_1^*$, then*

$$\frac{I_2^*}{S_2^*} < \frac{I_T}{S_2^*} < H_3 < H_1 < H_2 < \frac{I_T}{S_1^*} < \frac{I_1^*}{S_1^*};$$

(ii) If $I_2^* < I_1^* < I_T$, then

$$\frac{I_2^*}{S_2^*} < \frac{I_T}{S_2^*} < H_3 < H_2 < H_1, \quad \frac{I_T}{S_2^*} < \frac{I_T}{S_1^*} < H_2, \quad \frac{I_2^*}{S_2^*} < \frac{I_1^*}{S_1^*} < \frac{I_T}{S_1^*}.$$

Proof We just prove the case if $I_2^* < I_T < I_1^*$. When $I_T < I_2^* < I_1^*$ or $I_2^* < I_1^* < I_T$, the results can be obtained similarly by applying Proposition 3.4. By Proposition 3.4, there holds

$$I_2^* < I_T < I_1^* \iff H_3 < H_1 < H_2,$$

$$I_2^* < I_T \iff H_3 > \frac{I_T}{S_2^*} > \frac{I_2^*}{S_2^*},$$

$$I_T < I_1^* \iff H_2 < \frac{I_T}{S_1^*} < \frac{I_1^*}{S_2^*}.$$

Hence, the result is obtained following the above inequalities. □

3.3 Global dynamics

3.3.1 Case A.1: $I_T < I_2^* < I_1^*$

In this situation, E_1^V is a virtual equilibrium, whereas E_2^R is a real equilibrium. In this and the following analysis, we denote a possible real equilibrium by E_i^R and a possible virtual equilibrium by E_i^V , $i = 1, 2$, respectively. Furthermore, E_{p1} is never a pseudoequilibrium on $\Sigma_1 \subset \Omega_1$ by Proposition 3.1. For $\frac{I_T}{S_2^*} < \frac{I_2^*}{S_2^*} < \frac{I_1^*}{S_1^*}$, E_{p2} is never a pseudoequilibrium on $\Sigma_2 \subset \Omega_2$ by Proposition 3.3. We can obtain the globally asymptotical stability of E_2^R .

Theorem 3.3 E_2^R is globally asymptotically stable if $S_1^* < S_2^* < \frac{I_T}{\xi}$ and $I_T < I_2^* < I_1^*$.

- If $H_1 < H_3 < \frac{I_T}{S_2^*} < H_2 < \frac{I_T}{S_1^*} < \frac{I_1^*}{S_1^*}$, then there does not exist a sliding-mode domain on Ω_2 when $\xi < H_3$; the sliding-mode domain on Ω_2 is $\Sigma_2 = \{(S, I) \in \Omega_2 : \frac{I_T}{\xi} < S < S^+\}$ when $\xi > H_3$; as can be seen in Fig. 3(a);
- If $H_1 < H_3 < H_2 < \frac{I_T}{S_2^*} < \frac{I_T}{S_1^*} < \frac{I_1^*}{S_1^*}$, then there does not exist a sliding-mode domain on Ω_2 when $\xi < H_3$; the sliding-mode domain on Ω_2 is $\Sigma_2 = \{(S, I) \in \Omega_2 : \frac{I_T}{\xi} < S < S^+\}$ when $H_3 < \xi < H_2$; and $\Sigma_2 = \{(S, I) \in \Omega_2 : S^- < S < S^+\}$ when $\xi > H_2$; as can be seen in Fig. 3(b).

Proof The existence of limit cycles in regions G_1 and G_2 can be excluded by applying Dulac function $B = \frac{1}{SI}$. Note that the Dulac function cannot only be applicable to continuous systems but to systems with discontinuous right-hand side where the vector field is neither smooth nor continuous at the discontinuity surface, $I = I_T, S < \frac{I_T}{\xi}$ and $I = \xi S, S > \frac{I_T}{\xi}$ in system (1)–(2). In the following, to exclude the existence of the limit cycle, we extend the classic Dulac function to a modified one that avoids the sliding modes [22]. We redivide G_1 into two regions: $G_{11} = \{(S, I) \in G_1 : I < I_T\}$ and $G_{12} = \{(S, I) \in G_1 : I_T < I < \xi S\}$. By contradiction, suppose there exists a limit cycle Γ (as can be seen in Fig. 2) passing through the discontinuity surfaces Ω_1 and Ω_2 that surrounds the sliding mode Σ_1 and the real equilibrium E_2^R . Denote $\Gamma = \Gamma_1 + \Gamma_2 + \Gamma_3$, where $\Gamma_1 = \Gamma \cap G_{11}, \Gamma_2 = \Gamma \cap G_2, \Gamma_3 = \Gamma \cap G_{12}$. Let D be the bounded region divided by Γ and $D_1 = D \cap G_{11}, D_2 = D \cap G_2, D_3 = D \cap G_{12}$.

By doing the same in other subregions, we choose the Dulac function as $B = \frac{1}{SI}$. For better illustration and expression, denoting the dynamics in region G_{12} as governed by

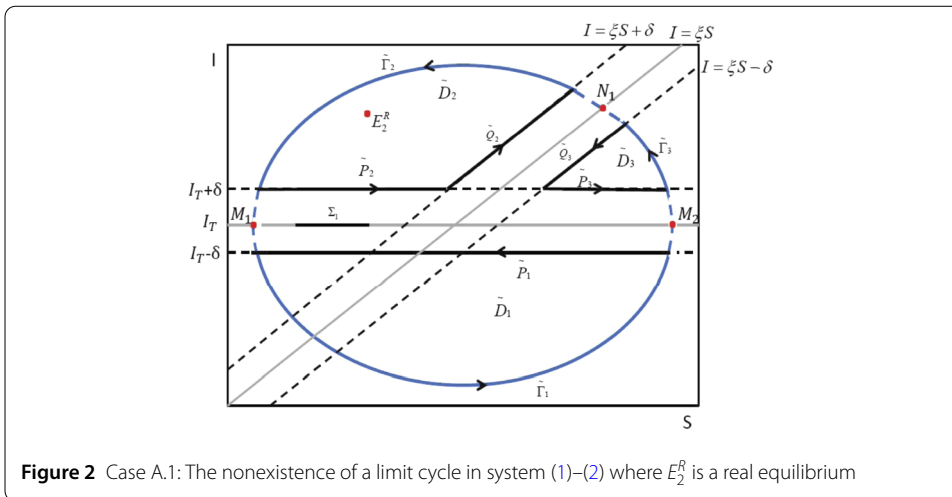


Figure 2 Case A.1: The nonexistence of a limit cycle in system (1)–(2) where E_2^R is a real equilibrium

$F_3(S, I) = F_1(S, I)$ (refer to Eq. (3)), we have

$$\sum_{i=1}^3 \left(\frac{\partial(BF_{i1})}{\partial S} + \frac{\partial(BF_{i2})}{\partial I} \right) = -\frac{3r}{KI} < 0.$$

Thus

$$\iint_{D_i} \left(\frac{\partial(Bf_1)}{\partial S} + \frac{\partial(Bf_2)}{\partial I} \right) dS dI = \sum_{i=1}^3 \iint_{D_i} \left(\frac{\partial(BF_{i1})}{\partial S} + \frac{\partial(BF_{i2})}{\partial I} \right) dS dI < 0.$$

Let \tilde{P}_i and \tilde{Q}_j be in the vicinity of the discontinuity surfaces Ω_1 and Ω_2 , and suppose \tilde{P}_i converges to $I = I_T$ and \tilde{Q}_j converges to $I = \xi S$ as δ approaches 0, $i = 1, 2, 3, j = 1, 2$. The corresponding bounded region D_i and Γ_i are relabeled as \tilde{D}_i and $\tilde{\Gamma}_i$, \tilde{D}_i and $\tilde{\Gamma}_i$ converge to D_i and Γ_i when $\delta \rightarrow 0$, $i = 1, 2, 3$, as can be seen in Fig. 2. Then we can obtain

$$\iint_{D_i} \left(\frac{\partial(BF_{i1})}{\partial S} + \frac{\partial(BF_{i2})}{\partial I} \right) dS dI = \lim_{\delta \rightarrow 0} \iint_{\tilde{D}_i} \left(\frac{\partial(BF_{i1})}{\partial S} + \frac{\partial(BF_{i2})}{\partial I} \right) dS dI.$$

Since $dS = F_{11} dt$ and $dI = F_{12} dt$ along $\tilde{\Gamma}_1$ and $dI = 0$ along \tilde{P}_1 , then in region \tilde{D}_1 we have the following result by applying Green’s theorem:

$$\begin{aligned} \iint_{\tilde{D}_1} \left(\frac{\partial(BF_{11})}{\partial S} + \frac{\partial(BF_{12})}{\partial I} \right) dS dI &= \oint_{\partial \tilde{D}_1} BF_{11} dI - BF_{12} dS \\ &= \int_{\tilde{\Gamma}_1} BF_{11} dI - BF_{12} dS + \int_{\tilde{P}_1} BF_{11} dI - BF_{12} dS \\ &= - \int_{\tilde{P}_1} BF_{12} dS. \end{aligned}$$

Similarly, in region \tilde{D}_2 where $dS = F_{21} dt$ and $dI = F_{22} dt$ along $\tilde{\Gamma}_2$ and $dI = 0$ along \tilde{P}_2 , $dI = \xi dS$ along \tilde{Q}_2 , we have

$$\iint_{\tilde{D}_2} \left(\frac{\partial(BF_{21})}{\partial S} + \frac{\partial(BF_{22})}{\partial I} \right) dS dI = \oint_{\partial \tilde{D}_2} BF_{21} dI - BF_{22} dS$$

$$\begin{aligned}
 &= \int_{\tilde{\Gamma}_2} BF_{21} dI - BF_{22} dS + \int_{\tilde{P}_2} BF_{21} dI - BF_{22} dS \\
 &\quad + \int_{\tilde{Q}_2} BF_{21} dI - BF_{22} dS \\
 &= - \int_{\tilde{P}_2} BF_{22} dS + \int_{\tilde{Q}_2} (\xi BF_{21} - BF_{22}) dS.
 \end{aligned}$$

In region \tilde{D}_3 where $dS = F_{11} dt$ and $dI = F_{12} dt$ along $\tilde{\Gamma}_3$ and $dI = 0$ along \tilde{P}_3 , $dI = \xi dS$ along \tilde{Q}_3 , we have

$$\iint_{\tilde{D}_3} \left(\frac{\partial(BF_{11})}{\partial S} + \frac{\partial(BF_{12})}{\partial I} \right) dS dI = - \int_{\tilde{P}_3} BF_{12} dS + \int_{\tilde{Q}_3} (\xi BF_{11} - BF_{12}) dS.$$

The intersection points of the limit cycle Γ and the line $I = I_T$ are denoted by $M_1 = (M_{11}, I_T)$ and $M_2 = (M_{21}, I_T)$, and the intersection point of Γ and the line $I = \xi S$ in region G_2 is denoted by $N_1 = (N_{11}, N_{12})$.

Since $c_2 > c_1$, $N_{11} > M_{11}$, and $\frac{I_T}{\xi} > M_{11}$, from the above discussions, we have

$$\begin{aligned}
 0 &> \sum_{i=1}^3 \iint_{D_i} \left(\frac{\partial(BF_{i1})}{\partial S} + \frac{\partial(BF_{i2})}{\partial I} \right) dS dI \\
 &= \lim_{\delta \rightarrow 0} \sum_{i=1}^3 \iint_{\tilde{D}_i} \left(\frac{\partial(BF_{i1})}{\partial S} + \frac{\partial(BF_{i2})}{\partial I} \right) dS dI \\
 &= \lim_{\delta \rightarrow 0} \left(- \int_{\tilde{P}_1} BF_{12} dS - \int_{\tilde{P}_2} BF_{22} dS + \int_{\tilde{Q}_2} (\xi BF_{21} - BF_{22}) dS \right. \\
 &\quad \left. - \int_{\tilde{P}_3} BF_{12} dS + \int_{\tilde{Q}_3} (\xi BF_{11} - BF_{12}) dS \right) \\
 &= - \int_{\frac{I_T}{\xi}}^{M_{11}} \left(\beta - \frac{\mu + d}{S} \right) dS - \int_{M_{11}}^{N_{11}} \left(\beta - \frac{\mu + d + c_2}{S} \right) dS \\
 &\quad - \int_{N_{11}}^{\frac{I_T}{\xi}} \left(\beta - \frac{\mu + d}{S} \right) dS - \int_{\frac{I_T}{\xi}}^{N_{11}} \frac{c_1}{S} dS \\
 &= -(\beta S - (\mu + d) \ln S) \Big|_{\frac{I_T}{\xi}}^{M_{11}} - (\beta S - (\mu + d + c_2) \ln S) \Big|_{M_{11}}^{N_{11}} \\
 &\quad - (\beta S - (\mu + d) \ln S) \Big|_{N_{11}}^{\frac{I_T}{\xi}} - c_1 \ln S \Big|_{\frac{I_T}{\xi}}^{N_{11}} \\
 &= (c_2 - c_1) \ln \frac{N_{11}}{M_{11}} + c_1 \ln \frac{\frac{I_T}{\xi}}{M_{11}} > 0,
 \end{aligned}$$

which is a contradiction. Hence, the existence of the limit cycle surrounding the sliding mode and the real equilibrium E_2^R is ruled out. Consequently, E_2^R is globally asymptotically stable. \square

Throughout this paper, in order to better present the solution trajectory, the vertical and horizontal nullclines of system (1)–(2) are shown by black dashed curves and black dashed–dotted lines, respectively. It can be easily seen that the curves $S = S_1^*$, $S = S_2^*$ are the

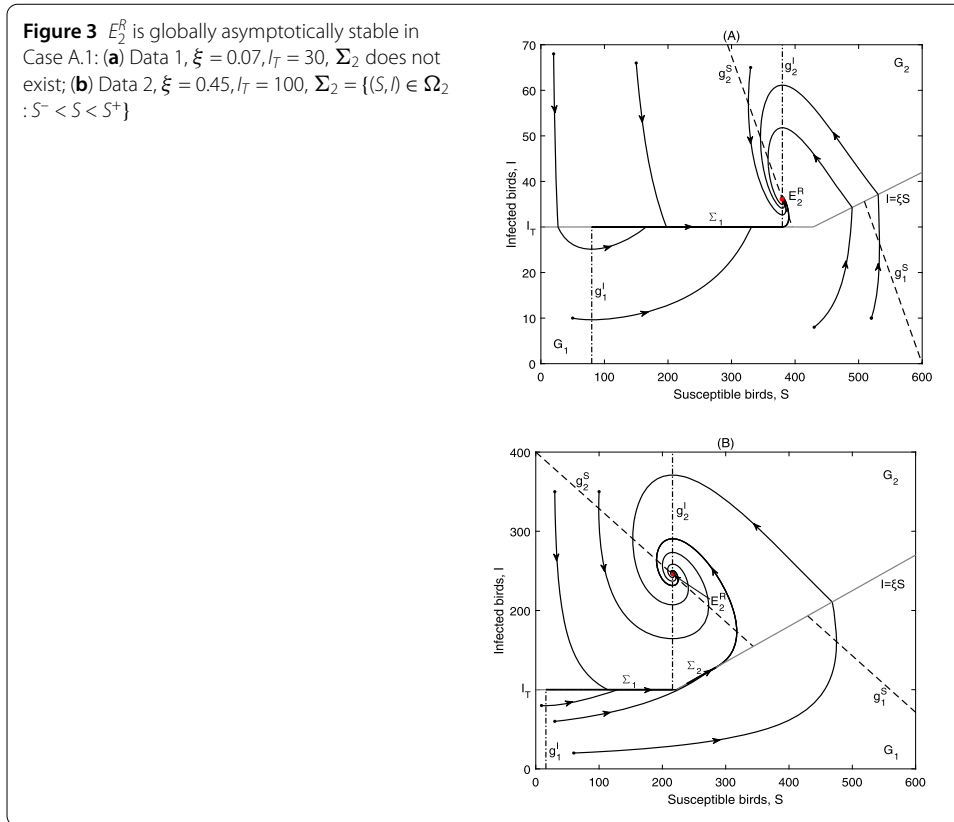


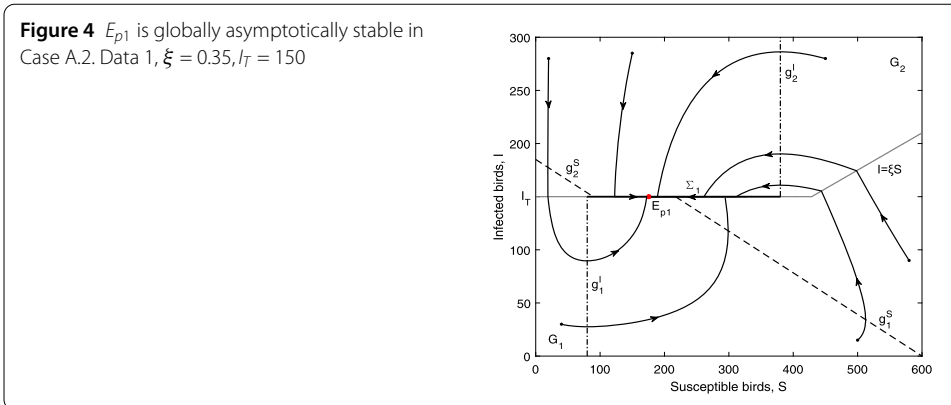
Table 1 Description of parameters in system (1)–(2)

Parameter	Definition	Data 1	Data 2	Data 3
r (/day)	Intrinsic growth rate of birds	0.0047	0.005	0.002
K (bird)	Maximal carrying capacity of the birds	600	700	700
μ (/day)	Natural death rate of birds	1.2×10^{-3}	1.2×10^{-4}	2.4×10^{-3}
d (/day)	Disease induced death rate of birds	4×10^{-4}	4×10^{-5}	2.2×10^{-4}
β (/day/bird)	Transmission rate from infected to susceptible birds	2×10^{-5}	1×10^{-5}	1×10^{-4}
c_1 (/day)	Culling rate of susceptible birds	0.001	0.001	0.001
c_2 (/day)	Culling rate of infected birds	0.006	0.002	0.002

horizontal nullclines of F_1 and F_2 , denoted by g_1^I and g_2^I , respectively. The curve $\{(S, I) \in G_1 : I = \frac{r}{\beta}(1 - \frac{S}{K})\}$ is the vertical nullcline of F_1 , denoted by g_1^S , while the curve $\{(S, I) \in G_2 : I = \frac{r}{\beta}(1 - \frac{S}{K}) - \frac{c_1}{\beta}\}$ is the vertical nullcline of F_2 , denoted by g_2^S .

The phase portrait in Case A.1 is shown in Fig. 3. Here we present the cases when the sliding-mode domain does not exist and when $\Sigma_2 = \{(S, I) \in \Omega_2 : S^- < S < S^+\}$, the case when $\Sigma_2 = \{(S, I) \in \Omega_2 : \frac{I_T}{\xi} < S < S^+\}$ is omitted here since it is similar. The solutions of system (1)–(2) will finally stabilize at E_2^R , which means the number of infected birds is eventually larger than the given threshold level, people will confront with an influenza pandemic which is intolerable and out of control. This departs from our target to control the disease. Hence, the threshold value I_T and ratio threshold value ξ are not a good choice.

In this and the following figures, we apply three different sets of parameter values for high quality figure display. All the parameter values have been used in [9, 12] and references therein, as can be seen in Table 1.



3.3.2 Case A.2: $I_2^* < I_T < I_1^*$

In this case, both E_1^V and E_2^V are virtual equilibria. Furthermore, $E_{p1} \in \Sigma_1 \subset \Omega_1$ is a pseudo-equilibrium according to Proposition 3.1. According to Propositions 3.2 and 3.5 and since $\xi < \frac{I_T}{S_2^*} < H_3$, there does not exist a sliding-mode domain on Ω_2 .

Similarly, by excluding the existence of the limit cycle as that in Theorem 3.3, we can derive the following result.

Theorem 3.4 E_{p1} is globally asymptotically stable if $S_1^* < S_2^* < \frac{I_T}{\xi}$ and $I_2^* < I_T < I_1^*$.

The solutions of system (1)–(2) with different initial values will all converge to the pseudo-equilibrium E_{p1} eventually. In this case, the influenza is controlled to the given threshold level I_T , as shown in Fig. 4.

3.3.3 Case A.3: $I_2^* < I_1^* < I_T$

In this case, E_1^R is a real equilibrium, whereas E_2^V is a virtual equilibrium. Moreover, E_{p1} is not a pseudo-equilibrium on $\Sigma_1 \subset \Omega_1$ by Proposition 3.1. Meanwhile, for $\frac{I_2^*}{S_2^*} < \frac{I_T}{S_2^*} < H_3 < H_2 < H_1$, by Proposition 3.2 and due to $\xi < \frac{I_T}{S_2^*}$, there does not exist a sliding-mode domain on Ω_2 . We can obtain the following result.

Theorem 3.5 E_1^R is globally asymptotically stable if $S_1^* < S_2^* < \frac{I_T}{\xi}$ and $I_2^* < I_1^* < I_T$.

All solutions of system (1)–(2) will stabilize at the level E_1^R below the threshold values, as shown in Fig. 5. In this case, the disease can be controlled to below the tolerance level in spite of a small endemic with size E_1^R .

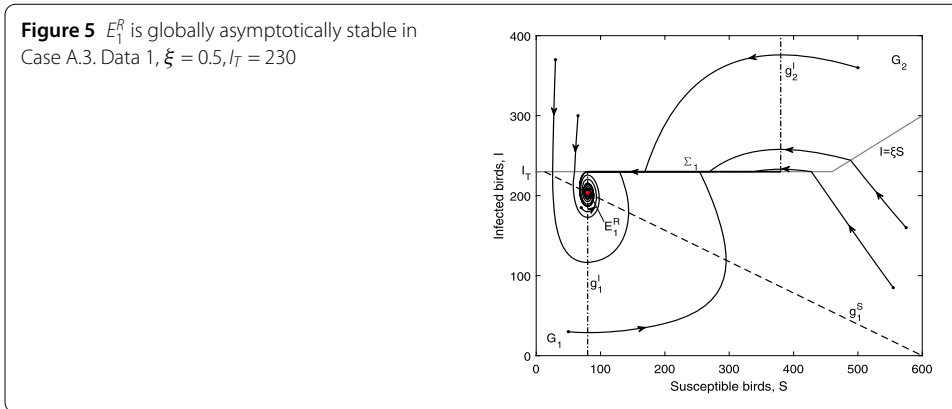
4 Case B: global dynamics when $S_1^* < \frac{I_T}{\xi} < S_2^*$ ($\frac{I_T}{S_2^*} < \xi < \frac{I_T}{S_1^*}$)

4.1 Sliding mode on Ω_1 and its dynamics

In this case, the sliding-mode domain on Ω_1 is

$$\Sigma_1 = \left\{ (S, I) \in \Omega_1 : S_1^* < S < \frac{I_T}{\xi} \right\}. \tag{8}$$

The sliding-mode dynamics on $\Sigma_1 \subset \Omega_1$ is represented by system (6). Furthermore, for the existence of the pseudo-equilibrium E_{p1} , we have the following result.



Proposition 4.1 E_{p1} is a pseudoequilibrium on $\Sigma_1 \subset \Omega_1$ if $S_1^* < S_{p1}^* < \frac{I_T}{\xi}$, that is, $I_2^* < I_T < I_1^*$, and $\frac{I_T}{S_2^*} < \xi < H_1$.

Proof Since $S_1^* < \frac{I_T}{\xi} < S_2^*$, E_{p1} becomes a pseudoequilibrium on $\Sigma_1 \subset \Omega_1$ if and only if $S_1^* < S_{p1}^* < \frac{I_T}{\xi}$, that is, $I_T < I_1^*$ and $\xi < \frac{I_T(\frac{r}{K} + \frac{c_1}{c_2}\beta)}{r + \frac{c_1}{c_2}(\mu+d) - \beta I_T} = H_1$. Proposition 3.5 indicates that $I_T > I_2^* \Leftrightarrow \frac{I_T}{S_2^*} < H_1, I_T < I_1^* \Leftrightarrow H_1 < \frac{I_T}{S_1^*}$. Then the result follows along with $\frac{I_T}{S_2^*} < \xi < \frac{I_T}{S_1^*}$. \square

4.2 Sliding mode on Ω_2 and its dynamics

In this case, the sliding-mode domain on Ω_2 and the conditions for E_{p2} to be a pseudoequilibrium on $\Sigma_2 \subset \Omega_2$ are related to the values of ξ and I_T , which can be referred to Propositions 3.2 and 3.3. The sliding-mode dynamics on $\Sigma_2 \subset \Omega_2$ can be represented by system (7).

4.3 Global dynamics

4.3.1 Case B.1: $I_T < I_2^* < I_1^*$

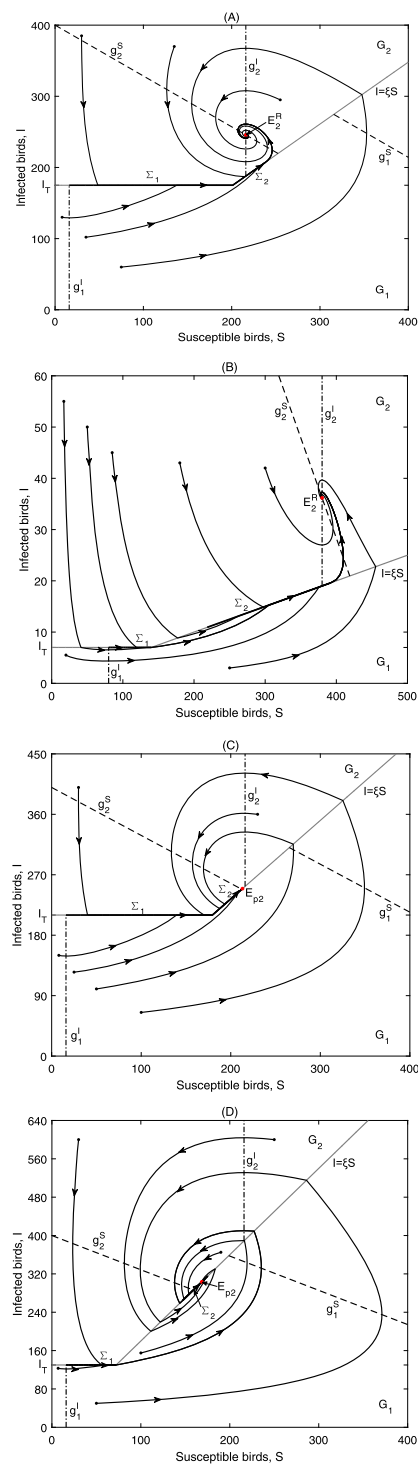
In Case B.1, E_1^V is a virtual equilibrium, E_2 is a real equilibrium if $\xi < \frac{I_2^*}{S_2^*}$, whilst E_2 is a virtual equilibrium if $\xi > \frac{I_2^*}{S_2^*}$. Furthermore, E_{p1} is not a pseudoequilibrium on Ω_1 by Proposition 4.1. According to Proposition 3.5, we have the following five different situations.

Theorem 4.1 Suppose $S_1^* < \frac{I_T}{\xi} < S_2^*$ and $I_T < I_2^* < I_1^*$, we have the following results:

- When $H_1 < H_3 < \frac{I_T}{S_2^*} < \frac{I_2^*}{S_2^*} < H_2 < \frac{I_T}{S_1^*} < \frac{I_1^*}{S_1^*}$, we have:
 - (i) If $\frac{I_T}{S_2^*} < \xi < \frac{I_2^*}{S_2^*}$, then E_2^R is a real equilibrium and is globally asymptotically stable; the sliding-mode domain on Ω_2 is $\Sigma_2 = \{(S, I) \in \Omega_2 : \frac{I_T}{\xi} < S < S^+\}$, and $E_{p2} \notin \Sigma_2 \subset \Omega_2$;
 - (ii) If $\frac{I_2^*}{S_2^*} < \xi < \frac{I_T}{S_1^*}$, then E_2^V is a virtual equilibrium, the sliding-mode domain on Ω_2 is $\Sigma_2 = \{(S, I) \in \Omega_2 : \frac{I_T}{\xi} < S < S^+\}$ when $\xi < H_2$, and $\Sigma_2 = \{(S, I) \in \Omega_2 : S^- < S < S^+\}$ when $\xi > H_2$, meanwhile $E_{p2} \in \Sigma_2 \subset \Omega_2$ is globally asymptotically stable; as can be seen in Fig. 6(c);
- When $H_1 < H_3 < \frac{I_T}{S_2^*} < H_2 < \frac{I_2^*}{S_2^*} < \frac{I_T}{S_1^*} < \frac{I_1^*}{S_1^*}$, we have:
 - (i) If $\frac{I_T}{S_2^*} < \xi < \frac{I_2^*}{S_2^*}$, then E_2^R is a real equilibrium and is globally asymptotically stable; the sliding-mode domain on Ω_2 is $\Sigma_2 = \{(S, I) \in \Omega_2 : \frac{I_T}{\xi} < S < S^+\}$ when $\xi < H_2$,

Figure 6 E_2^R is globally asymptotically stable in Case B.1:

(a) Data 2, $\xi = 0.87, I_T = 175, \Sigma_2 = \{(S, I) \in \Omega_2 : \frac{I_T}{\xi} < S < S^+\}$; (b) Data 1, $\xi = 0.05, I_T = 7, \Sigma_2 = \{(S, I) \in \Omega_2 : S^- < S < S^+\}$; E_{p2} is globally asymptotically stable in Case B.1: (c) Data 2, $\xi = 1.17, I_T = 210, \Sigma_2 = \{(S, I) \in \Omega_2 : \frac{I_T}{\xi} < S < S^+\}$; (d) Data 2, $\xi = 1.8, I_T = 130, \Sigma_2 = \{(S, I) \in \Omega_2 : S^- < S < S^+\}$



- and $\Sigma_2 = \{(S, I) \in \Omega_2 : S^- < S < S^+\}$ when $\xi > H_2$, meanwhile $E_{p2} \notin \Sigma_2 \subset \Omega_2$; as can be seen in Fig. 6(a);
- (ii) If $\frac{I_2^*}{S_2^*} < \xi < \frac{I_T}{S_1^*}$, then E_2^V is a virtual equilibrium, the sliding-mode domain on Ω_2 is $\Sigma_2 = \{(S, I) \in \Omega_2 : S^- < S < S^+\}$, meanwhile $E_{p2} \in \Sigma_2 \subset \Omega_2$ is globally asymptotically stable;

- When $H_1 < H_3 < \frac{I_T}{S_2^*} < H_2 < \frac{I_T}{S_1^*} < \frac{I_2^*}{S_2^*} < \frac{I_1^*}{S_1^*}$, we have that E_2^R is a real equilibrium and is globally asymptotically stable; the sliding-mode domain on Ω_2 is $\Sigma_2 = \{(S, I) \in \Omega_2 : \frac{I_T}{\xi} < S < S^+\}$ when $\xi < H_2$, and $\Sigma_2 = \{(S, I) \in \Omega_2 : S^- < S < S^+\}$ when $\xi > H_2$, meanwhile $E_{p2} \notin \Sigma_2 \subset \Omega_2$; as can be seen in Fig. 6(b);
- When $H_1 < H_3 < H_2 < \frac{I_T}{S_2^*} < \frac{I_T}{S_1^*} < \frac{I_2^*}{S_2^*} < \frac{I_1^*}{S_1^*}$, we have that E_2^R is a real equilibrium and is globally asymptotically stable; the sliding-mode domain on Ω_2 is $\Sigma_2 = \{(S, I) \in \Omega_2 : S^- < S < S^+\}$, meanwhile $E_{p2} \notin \Sigma_2 \subset \Omega_2$;
- When $H_1 < H_3 < H_2 < \frac{I_T}{S_2^*} < \frac{I_2^*}{S_2^*} < \frac{I_T}{S_1^*} < \frac{I_1^*}{S_1^*}$, we have:
 - (i) If $\frac{I_T}{S_2^*} < \xi < \frac{I_2^*}{S_2^*}$, then E_2^R is a real equilibrium and is globally asymptotically stable; the sliding-mode domain on Ω_2 is $\Sigma_2 = \{(S, I) \in \Omega_2 : S^- < S < S^+\}$, $E_{p2} \notin \Sigma_2 \subset \Omega_2$;
 - (ii) If $\frac{I_2^*}{S_2^*} < \xi < \frac{I_T}{S_1^*}$, then E_2^V is a virtual equilibrium, the sliding-mode domain on Ω_2 is $\Sigma_2 = \{(S, I) \in \Omega_2 : S^- < S < S^+\}$, meanwhile $E_{p2} \in \Sigma_2 \subset \Omega_2$ is globally asymptotically stable; as can be seen in Fig. 6(d).

The solutions of system (1)–(2) in this case will finally stabilize either at E_2^R or E_{p2} with different sliding-mode domains $\Sigma_2 \subset \Omega_2$, as can be seen in Fig. 6. The disease will persist at an intolerable level or be controlled at the given level. Note that we do not show all the figures, for others are similar with the given ones.

4.3.2 Case B.2: $I_2^* < I_T < I_1^*$

In this case, both E_1^V and E_2^V are virtual equilibria; E_{p1} is a pseudoequilibrium if $\frac{I_T}{S_2^*} < \xi < H_1$. For $\frac{I_2^*}{S_2^*} < \frac{I_T}{S_2^*} < H_3 < H_1 < H_2 < \frac{I_T}{S_1^*} < \frac{I_1^*}{S_1^*}$ when $I_2^* < I_T < I_1^*$, hence, we have the following results.

Theorem 4.2 Suppose $S_1^* < \frac{I_T}{\xi} < S_2^*$ and $I_2^* < I_T < I_1^*$, we have:

- (i) If $\frac{I_T}{S_2^*} < \xi < H_1$, then $E_{p1} \in \Sigma_1 \subset \Omega_1$ is globally asymptotically stable; there is no sliding mode on Ω_2 when $\xi < H_3$, the sliding-mode domain on Ω_2 is $\Sigma_2 = \{(S, I) \in \Omega_2 : \frac{I_T}{\xi} < S < S^+\}$ when $\xi > H_3$, meanwhile $E_{p2} \notin \Sigma_2 \subset \Omega_2$; as can be seen in Fig. 7(a)–(b);
- (ii) If $H_1 < \xi < \frac{I_T}{S_1^*}$, then $E_{p1} \notin \Sigma_1 \subset \Omega_1$, the sliding-mode domain on Ω_2 is $\Sigma_2 = \{(S, I) \in \Omega_2 : \frac{I_T}{\xi} < S < S^+\}$ when $\xi < H_2$, and $\Sigma_2 = \{(S, I) \in \Omega_2 : S^- < S < S^+\}$ when $\xi > H_2$, meanwhile $E_{p2} \in \Sigma_2 \subset \Omega_2$ is globally asymptotically stable; as can be seen in Fig. 7(c)–(d).

In this case, the number of infected birds will finally converge to a level equal to the given threshold value, which indicates the disease is controlled from the biological point of view.

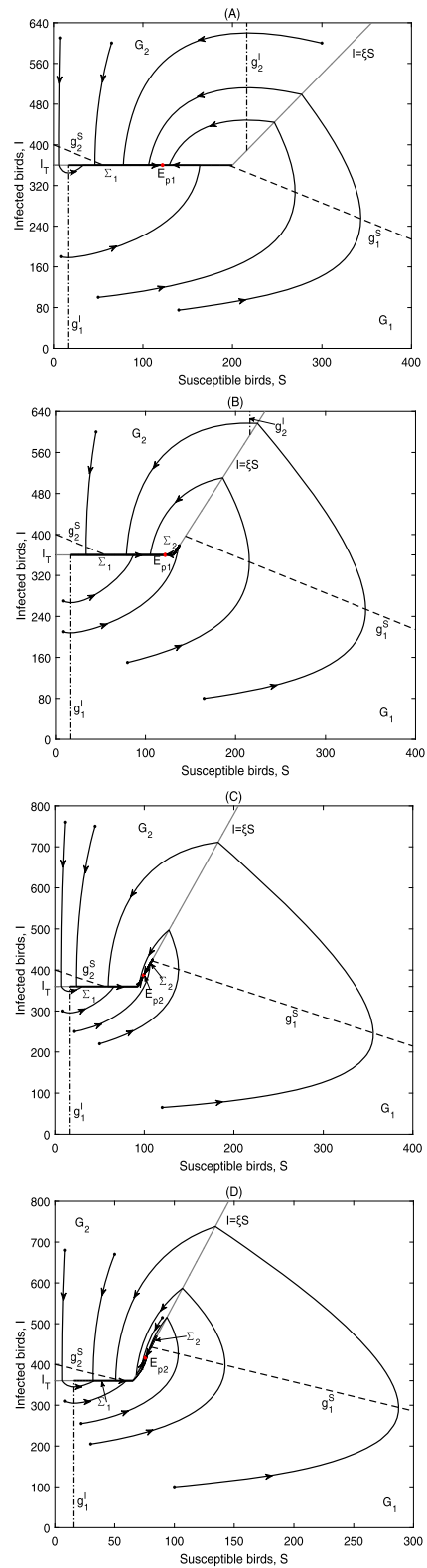
4.3.3 Case B.3: $I_2^* < I_1^* < I_T$

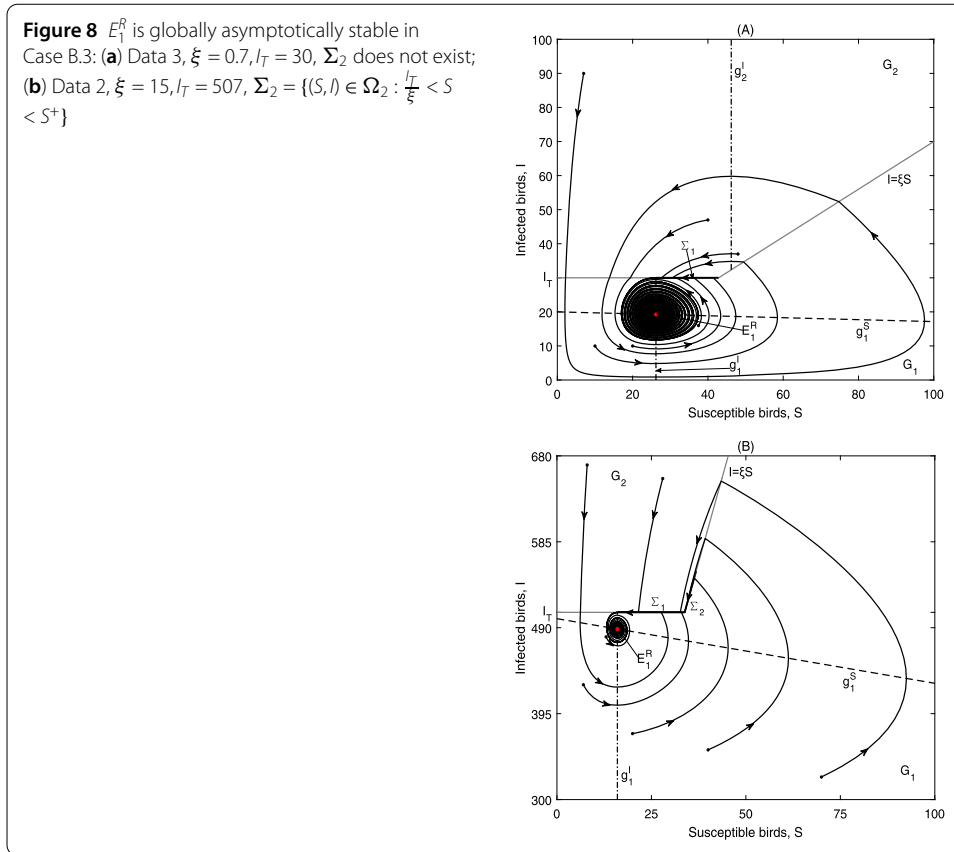
In this case, E_1^R is a real equilibrium, while E_2^V is a virtual equilibrium; E_{p1} is not a pseudoequilibrium on Ω_1 by Proposition 4.1. We have the following results by Proposition 3.5.

Theorem 4.3 Suppose $S_1^* < \frac{I_T}{\xi} < S_2^*$ and $I_2^* < I_1^* < I_T$. Then E_1^R is globally asymptotically stable, and:

- When $\frac{I_2^*}{S_2^*} < \frac{I_T}{S_2^*} < \frac{I_T}{S_1^*} < H_3 < H_2 < H_1$, there is no sliding mode on Ω_2 as can be seen in Fig. 8(a);

Figure 7 E_{p1} is globally asymptotically stable in Case B.2: **(a)** Data 2, $\xi = 1.8, I_T = 360, \Sigma_2$ does not exist; **(b)** Data 2, $\xi = 2.75, I_T = 360, \Sigma_2 = \{(S, I) \in \Omega_2 : \frac{I_T}{\xi} < S < S^+\}$; E_{p2} is globally asymptotically stable in Case B.2: **(c)** Data 2, $\xi = 3.9, I_T = 360, \Sigma_2 = \{(S, I) \in \Omega_2 : \frac{I_T}{\xi} < S < S^+\}$; **(d)** Data 2, $\xi = 5.5, I_T = 360, \Sigma_2 = \{(S, I) \in \Omega_2 : S^- < S < S^+\}$





- When $\frac{I_T^*}{S_2^*} < \frac{I_T}{S_2^*} < H_3 < \frac{I_T}{S_1^*} < H_2 < H_1$, there is no sliding mode on Ω_2 if $\xi < H_3$ and $\Sigma_2 = \{(S, I) \in \Omega_2 : \frac{I_T}{\xi} < S < S^+\}$ if $\xi > H_3$, meanwhile $E_{p2} \notin \Sigma_2 \subset \Omega_2$; as can be seen in Fig. 8(b).

As in Case A.3, all solutions will finally stabilize at a level below the infected threshold level I_T , as can be seen in Fig. 8, which shows the disease is controlled below a tolerance level.

5 Case C: global dynamics when $\frac{I_T}{\xi} < S_1^* < S_2^*$ ($\xi > \frac{I_T}{S_1^*}$)

5.1 Sliding mode on Ω_1 and its dynamics

In this case since $\frac{I_T}{\xi} < S_1^*$, there does not exist a sliding-mode domain on Ω_1 .

5.2 Sliding mode on Ω_2 and its dynamics

As in Case B, the sliding-mode domain on Ω_2 and the conditions for E_{p2} to be a pseudo-equilibrium on $\Sigma_2 \subset \Omega_2$ are related to the values of ξ and I_T , which can be referred to Propositions 3.2 and 3.3. The sliding-mode dynamics on $\Sigma_2 \subset \Omega_2$ can be represented by system (7).

5.3 Global dynamics

5.3.1 Case C.1: $I_T < I_2^* < I_1^*$

In this situation, E_1 is a real equilibrium if $\xi > \frac{I_1^*}{S_1^*}$, whilst E_1 is a virtual equilibrium if $\xi < \frac{I_1^*}{S_1^*}$; E_2 is a real equilibrium if $\xi < \frac{I_2^*}{S_2^*}$, whilst E_2 is a virtual equilibrium if $\xi > \frac{I_2^*}{S_2^*}$. By Proposition 3.5, we have the following results.

Theorem 5.1 *Suppose $S_1^* < S_2^* < \frac{I_T}{\xi}$ and $I_T < I_2^* < I_1^*$. Then the sliding-mode domain on Ω_2 is $\Sigma_2 = \{(S, I) \in \Omega_2 : S^- < S < S^+\}$ for $\frac{I_T}{S_1^*} > H_2$, and:*

- *When $H_1 < H_3 < \frac{I_T}{S_2^*} < \frac{I_2^*}{S_2^*} < \frac{I_T}{S_1^*} < \frac{I_1^*}{S_1^*}$, one has:*
 - (i) *If $\frac{I_T}{S_1^*} < \xi < \frac{I_1^*}{S_1^*}$, both E_1^V and E_2^V are virtual equilibria; $E_{p2} \in \Sigma_2 \subset \Omega_2$ is globally asymptotically stable; the figure is similar to Fig. 9(b);*
 - (ii) *If $\xi > \frac{I_1^*}{S_1^*}$, E_1^R is a real equilibrium, while E_2^V is a virtual equilibrium; E_1^R is globally asymptotically stable, meanwhile $E_{p2} \notin \Sigma_2 \subset \Omega_2$; the figure is similar to Fig. 9(c);*
- *When $H_1 < H_3 < \frac{I_T}{S_2^*} < \frac{I_T}{S_1^*} < \frac{I_2^*}{S_2^*} < \frac{I_1^*}{S_1^*}$, one has*
 - (i) *If $\frac{I_T}{S_1^*} < \xi < \frac{I_2^*}{S_2^*}$, E_1^V is a virtual equilibrium, while E_2^R is a real equilibrium; E_2^R is globally asymptotically stable, meanwhile $E_{p2} \notin \Sigma_2 \subset \Omega_2$ as can be seen in Fig. 9(a);*
 - (ii) *If $\frac{I_2^*}{S_2^*} < \xi < \frac{I_1^*}{S_1^*}$, both E_1^V and E_2^V are virtual equilibria; $E_{p2} \in \Sigma_2 \subset \Omega_2$ is globally asymptotically stable as can be seen in Fig. 9(b);*
 - (iii) *If $\xi > \frac{I_1^*}{S_1^*}$, E_1^R is a real equilibrium, while E_2^V is a virtual equilibrium; E_1^R is globally asymptotically stable, meanwhile $E_{p2} \notin \Sigma_2 \subset \Omega_2$ as can be seen in Fig. 9(c).*

In this case, all solutions of system (1)–(2) rely greatly on the combinations of I_T and ξ . The solutions should converge to E_2^R, E_{p2} or E_1^R as can be seen in Fig. 9, which then leads to different control outcomes. Therefore an efficient threshold policy is essential by driving the number of infected birds below a given level or at a tolerance level.

5.3.2 Case C.2: $I_2^* < I_T < I_1^*$

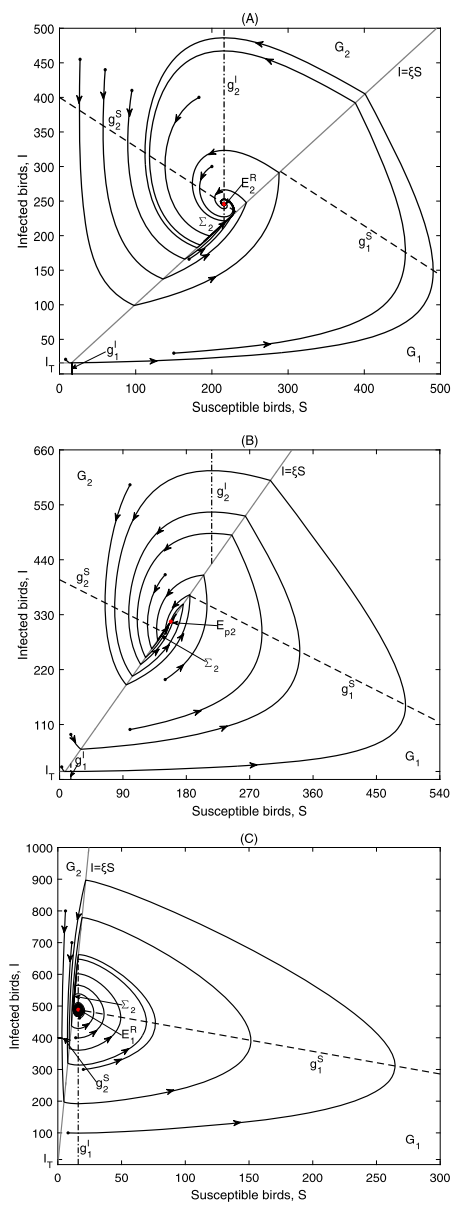
In this case, for $\frac{I_2^*}{S_2^*} < \frac{I_T}{S_2^*} < H_3 < H_1 < H_2 < \frac{I_T}{S_1^*} < \frac{I_1^*}{S_1^*}$ and $\xi > \frac{I_T}{S_1^*}$, then $\xi > \frac{I_2^*}{S_2^*}$ and E_2 is a virtual equilibrium, denoted by E_2^V ; E_1 is a real equilibrium if $\xi > \frac{I_1^*}{S_1^*}$, whilst E_1 is a virtual equilibrium if $\xi < \frac{I_1^*}{S_1^*}$.

Theorem 5.2 *Suppose $S_1^* < S_2^* < \frac{I_T}{\xi}$ and $I_2^* < I_T < I_1^*$. Then the sliding-mode domain on Ω_2 is $\Sigma_2 = \{(S, I) \in \Omega_2 : S^- < S < S^+\}$ for $H_2 < \frac{I_T}{S_1^*}$, and:*

- (i) *If $\frac{I_T}{S_1^*} < \xi < \frac{I_1^*}{S_1^*}$, E_1^V is a virtual equilibrium. $E_{p2} \in \Sigma_2 \subset \Omega_2$ is globally asymptotically stable as can be seen in Fig. 10(a);*
- (ii) *If $\xi > \frac{I_1^*}{S_1^*}$, E_1^R is a real equilibrium and is globally asymptotically stable, meanwhile $E_{p2} \notin \Sigma_2 \subset \Omega_2$ as can be seen in Fig. 10(b).*

As can be seen in Fig. 10, all solutions of the system will finally stabilize at either E_{p2} or E_1^R , the level equal to or below the given threshold level, and then the influenza is controlled below or at a tolerance level.

Figure 9 Global dynamics in Case C.1: (a) E_2^R is globally asymptotically stable. Data 2, $\xi = 1.01$, $I_T = 16$; (b) E_{p2} is globally asymptotically stable. Data 2, $\xi = 2$, $I_T = 16$; (c) E_1^R is globally asymptotically stable. Data 2, $\xi = 41$, $I_T = 16$

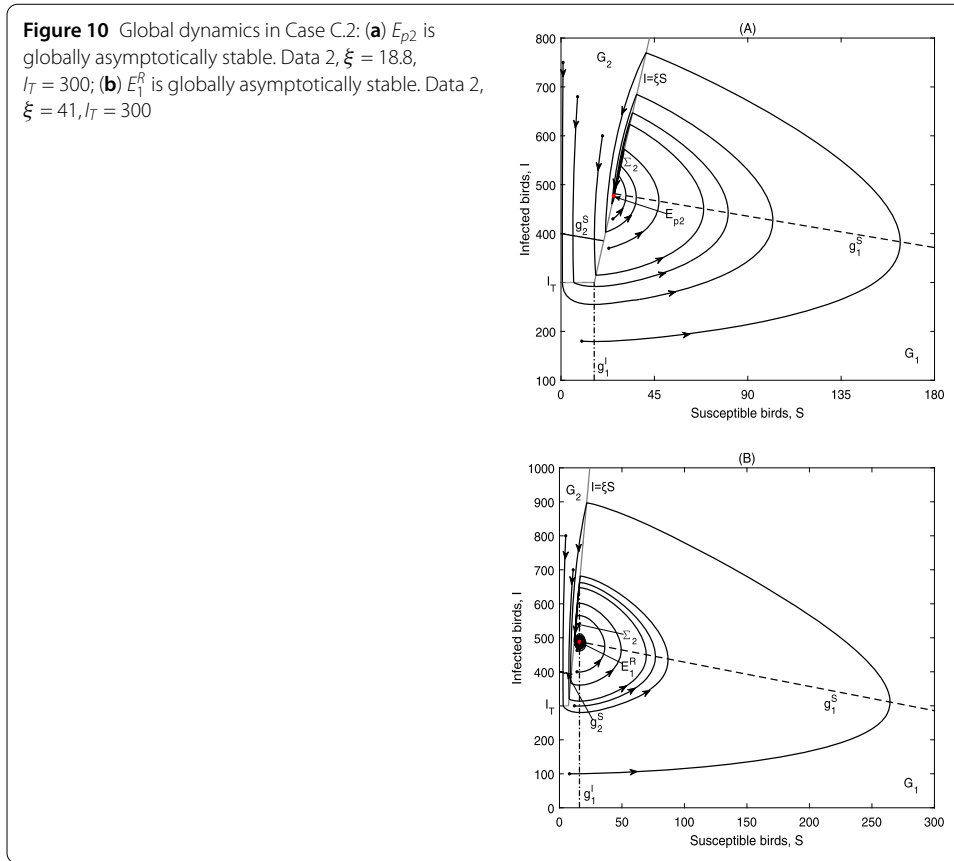


5.3.3 Case C.3: $I_2^* < I_1^* < I_T$

In this case, E_1^R is a real equilibrium, E_2^V is a virtual equilibrium. By Proposition 3.5, we have the following result.

Theorem 5.3 Suppose $S_1^* < S_2^* < \frac{I_T}{\xi}$ and $I_2^* < I_1^* < I_T$, then E_1^R is globally asymptotically stable, and for $\frac{I_2^*}{S_1^*} < \frac{I_T}{S_1^*}$ we have:

- When $\frac{I_2^*}{S_2^*} < \frac{I_T}{S_2^*} < \frac{I_T}{S_1^*} < H_3 < H_2 < H_1$, there does not exist a sliding-mode domain if $\xi < H_3$, the sliding-mode domain on Ω_2 is $\Sigma_2 = \{(S, I) \in \Omega_2 : \frac{I_T}{\xi} < S < S^+\}$ if $H_3 < \xi < H_2$, and $\Sigma_2 = \{(S, I) \in \Omega_2 : S^- < S < S^+\}$ if $\xi > H_2$, meanwhile $E_{p2} \notin \Sigma_2 \subset \Omega_2$ as can be seen in Fig. 11(a)–(b);



- When $\frac{I_T^*}{S_2^*} < \frac{I_T}{S_2} < H_3 < \frac{I_T}{S_1} < H_2 < H_1$, the sliding-mode domain on Ω_2 is $\Sigma_2 = \{(S, I) \in \Omega_2 : \frac{I_T}{\xi} < S < S^+\}$ if $\xi < H_2$, and $\Sigma_2 = \{(S, I) \in \Omega_2 : S^- < S < S^+\}$ if $\xi > H_2$, meanwhile $E_{p2} \notin \Sigma_2 \subset \Omega_2$; the figures are similar to Fig. 11(a)–(b).

The outcomes in this case achieve our objective as shown in Fig. 11, that is, to drive the number of infected birds to a level below the tolerance level. We could choose the corresponding threshold values in practice.

6 Conclusion and discussion

In this work, we proposed and analyzed an avian-only Filippov model, which is governed by nonlinear ordinary differential equations with discontinuous right-hand sides and a nonsmooth separation line. On the one hand, it is generally impossible to completely depopulate the infected birds, nor it is economically or biologically feasible. So when carrying out control strategies, the objective is to drive the number of infected birds to a tolerance or available level. On the other hand, when the interaction ratio of the numbers of infected and susceptible birds is below a ratio threshold value ξ , in order to maximize the economic profits, more effort can be saved by taking no control measures. In Sects. 3–5, it is shown that the solutions of system (1)–(2) will finally stabilize at either one of the two endemic equilibria in each subregion or the sliding equilibria on the two sliding modes. The results indicate that we can choose a suitable tolerance threshold I_T and/or a suitable ratio threshold ξ such that system (1)–(2) finally approaches E_1 in G_1 or a sliding equi-

Figure 11 E_1^R is globally asymptotically stable in Case C.3: (a) Data 3, $\xi = 1.16, I_T = 30$. Σ_2 does not exist; (b) Data 3, $\xi = 1.9, I_T = 30$, $\Sigma_2 = \{(S, I) \in \Omega_2 : \frac{I_T}{\xi} < S < S^+\}$

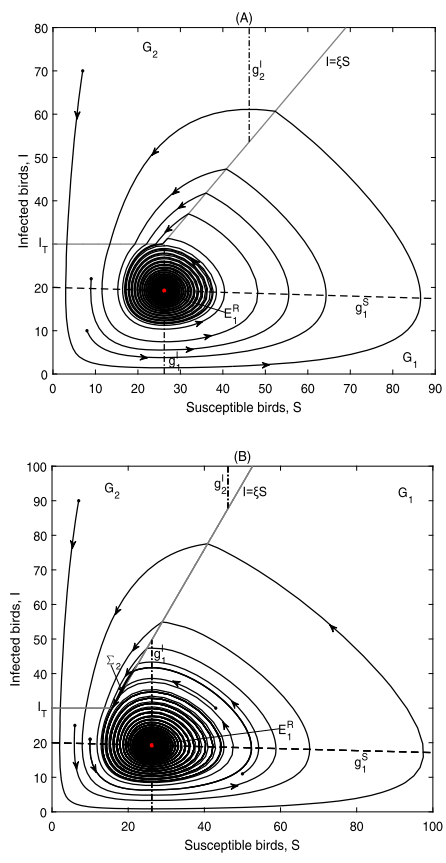


Table 2 Global dynamics of system (1)–(2) summarized from Sects. 3, 4, and 5

Case	Condition	Equilibrium	Main result
$S_1^* < S_2^* < \frac{I_T}{\xi}$	$I_T < I_2^* < I_1^*$	E_1^Y, E_2^R	(II)
$S_1^* < S_2^* < \frac{I_T}{\xi}$	$I_2^* < I_T < I_1^*$	E_1^Y, E_2^Y, E_{p1}	(III)
$S_1^* < S_2^* < \frac{I_T}{\xi}$	$I_2^* < I_1^* < I_T$	E_1^R, E_2^Y	(I)
$S_1^* < \frac{I_T}{\xi} < S_2^*$	$I_T < I_2^* < I_1^*, \xi < \frac{I_2^*}{S_2^*}$	E_1^Y, E_2^R	(II)
$S_1^* < \frac{I_T}{\xi} < S_2^*$	$I_T < I_2^* < I_1^*, \xi > \frac{I_2^*}{S_2^*}$	E_1^Y, E_2^Y, E_{p2}	(III)
$S_1^* < \frac{I_T}{\xi} < S_2^*$	$I_2^* < I_T < I_1^*, \xi < H_1$	E_1^Y, E_2^Y, E_{p1}	(III)
$S_1^* < \frac{I_T}{\xi} < S_2^*$	$I_2^* < I_T < I_1^*, \xi > H_1$	E_1^Y, E_2^Y, E_{p2}	(III)
$S_1^* < \frac{I_T}{\xi} < S_2^*$	$I_2^* < I_1^* < I_T$	E_1^R, E_2^Y	(I)
$\frac{I_T}{\xi} < S_1^* < S_2^*$	$I_T < I_2^* < I_1^*, \xi < \frac{I_2^*}{S_2^*}$	E_1^Y, E_2^R	(II)
$\frac{I_T}{\xi} < S_1^* < S_2^*$	$I_T < I_2^* < I_1^*, \frac{I_2^*}{S_2^*} < \xi < \frac{I_1^*}{S_1^*}$	E_1^Y, E_2^Y, E_{p2}	(III)
$\frac{I_T}{\xi} < S_1^* < S_2^*$	$I_T < I_2^* < I_1^*, \xi > \frac{I_1^*}{S_1^*}$	E_1^R, E_2^Y	(I)
$\frac{I_T}{\xi} < S_1^* < S_2^*$	$I_2^* < I_T < I_1^*, \xi < \frac{I_1^*}{S_1^*}$	E_1^Y, E_2^Y, E_{p2}	(III)
$\frac{I_T}{\xi} < S_1^* < S_2^*$	$I_2^* < I_T < I_1^*, \xi > \frac{I_1^*}{S_1^*}$	E_1^R, E_2^Y	(I)
$\frac{I_T}{\xi} < S_1^* < S_2^*$	$I_2^* < I_1^* < I_T$	E_1^R, E_2^Y	(I)

librium E_{pi} on $\Sigma_i \subset \Omega_i, i = 1, 2$, and then our objective, that is, inhibiting the infection or stabilizing the infection to a desirable level, is obtained. The main analytical results are summarized in Table 2, with the following biological implications.

- (I) The system (1)–(2) has a unique globally asymptotically stable equilibrium E_1^R , as illustrated in Figs. 5, 8, 9(c), 10(b), 11. The number of infected birds will finally stabilize at a level below the given threshold. Hence, in this situation, the influenza could be controlled below a given level in spite of a small endemic with size E_1^R . In practice, these choices of threshold values are preferable.
- (II) The system (1)–(2) has a unique globally asymptotically stable equilibrium E_2^R , as can be seen in Figs. 3, 6(a)–(b), 9(a). For these choices of threshold levels, the number of infected birds will converge to a high level above the threshold values, and then the avian influenza may be out of control by persisting at an intolerable level E_2^R .
- (III) There is a globally asymptotically stable pseudoequilibrium E_{p1} or E_{p2} . So the number of infected birds will eventually approach the given threshold values, as can be seen in Figs. 6(c)–(d), 7, 9(b), 10(a). The influenza is finally controlled at a tolerance level.

Note that our objective is to maintain the number of infected birds not exceeding a desired level. The analytical results show that the choice of the infected threshold value I_T and the ratio threshold ξ is of great significance to lead the number of the infected birds to an acceptable level. For Cases (I) and (III), our control objective can be achieved since the eventual number of the infected birds is equal to or below the given threshold levels. However, the number of the infected birds will be above the separation line eventually in Case (II), which is not our desire since tremendous economic damage will be caused. The findings could be beneficial to decide whether and when to take control strategies based on these two threshold values.

The threshold policy adopted by Chong et al. [25] treats the infected birds as an index. However, when the number of infected birds is relatively small compared to the number of susceptible birds, economic considerations may be more important than the disease control. Hence, a threshold policy considering both the number of infected birds and the interaction ratio of the numbers of infected and susceptible birds may be more realistic from the economical point of view. On the other hand, compared with the model proposed by Chong et al. [25] ($\xi = 0$ in system (1)–(2) with constant growth for the susceptible birds), we find that if the values of I_T and/or ξ are chosen to satisfy $S_2^* < \frac{I_T}{\xi}$ or $I_T > I_1^*$, then both models present the same results, that is, the disease persists at the level of E_2 when $I_T < I_2^*$, the number of infected birds stays at the available level E_{p1} when $I_2^* < I_T < I_1^*$, and the influenza is totally in control by stabilizing at E_1 when $I_T > I_1^*$. However, when the number of susceptible and/or infected birds is large enough, system (1)–(2) shows more complex dynamics. For example, in Case C.1 when $\frac{I_T}{\xi} < S_1^* < S_2^*$ and $I_T < I_2^*$, the solutions could converge to E_2^R, E_{p2} or E_1^R , resulting in different control outcomes, which shows the importance of the number of susceptible birds and the interaction ratio of the infected and susceptible birds in disease control.

Also, in [38] and our previous work [9], the authors considered a two-threshold policy in combating avian influenza. That is, culling of infected and/or susceptible birds depends on whether the number of infected (susceptible) birds exceeds the infected (susceptible) threshold level or not. The results show that if the susceptible threshold level is chosen to be large enough while the infected threshold level is chosen to be small enough, then the disease may persist at an intolerable level. While system (1)–(2) in this case indicates that the disease could be controlled to below the tolerance level. Hence taking the interaction

ratio of the infected and susceptible birds into consideration may be of some importance. Therefore, the avian-only model with a nonsmooth separation line proposed in this work may provide some new threshold policies in avian influenza control.

The theoretical results obtained in this work show that by choosing an appropriate threshold policy with a suitable tolerance threshold I_T and/or a suitable ratio threshold ξ , we can finally drive the influenza below or to be equal to the given tolerance level. It is worth noting that depopulation of susceptible and/or infected birds can still be triggered to stop the infection from progressing to an intolerable pandemic. Therefore an effective and efficient threshold policy is essential to control the influenza by driving the number of infected birds below or to a chosen level.

Acknowledgements

Not applicable.

Funding

National Natural Science Foundation of China (NSFC 11401349) and the Foundation for Outstanding Young Scientist in Shandong Province (BS2014SF008).

Availability of data and materials

Not applicable.

Competing interests

The authors declare that they have no competing interests.

Authors' contributions

In this research work, YY contributed to analysis and manuscript preparation. JW performed the numerical simulations. All authors read and approved the final manuscript.

Publisher's Note

Springer Nature remains neutral with regard to jurisdictional claims in published maps and institutional affiliations.

Received: 8 December 2020 Accepted: 12 April 2021 Published online: 20 April 2021

References

1. Alexander, J.D.: An overview of the epidemiology of avian influenza. *Vaccine* **25**, 5637–5644 (2007)
2. Alexander, J.D.: A review of avian influenza in different bird species. *Vet. Microbiol.* **74**, 3–13 (2000)
3. Peiris, J.S., de Jong, M.D., Guan, Y.: Avian influenza virus (H5N1): a threat to human health. *Clin. Microbiol. Rev.* **20**, 243–267 (2007)
4. Smith, G.J., Bahl, J., Vijaykrishna, D., Zhang, J., Poon, L.M., Chen, H., et al.: Dating the emergence of pandemic influenza viruses. *Proc. Natl. Acad. Sci.* **106**, 11709–11712 (2009)
5. Zilberman, D., Otte, J., Roland-Host, D., Pfeiffer, D.: The cost of saving a statistical life: a case for influenza prevention and control. *Nat. Resour. Manag. Policy* **36**, 135–141 (2012)
6. Li, Q., Zhou, L., Zhou, M., Chen, Z., Li, F., Wu, H., et al.: Epidemiology of human infections with avian influenza A(H7N9) virus in China. *N. Engl. J. Med.* **370**(6), 520–532 (2014)
7. He, Y., Liu, P., Tang, S., Chen, Y., Pei, E., Zhao, B., et al.: Live poultry market closure and control of avian influenza A(H7N9), Shanghai, China. *Emerg. Infect. Dis.* **20**(9), 1565–1566 (2014)
8. Perez, D.R., Garcia-Sastre, A.: H5N1, a wealth of knowledge to improve pandemic preparedness. *Virus Res.* **178**, 1–2 (2013)
9. Yang, Y., Wang, L.: Global dynamics and rich sliding motion in an avian-only Filippov system in combating avian influenza. *Int. J. Bifurc. Chaos* **30**(1), 2050008 (2020)
10. Avian Influenza-Questions & Answers Tech. Rep.: Animal Production and Health Division. <http://www.fao.org/avianflu/en/qanda.html#7> (2018)
11. Mu, R., Yang, Y.: Global dynamics of an avian influenza A(H7N9) epidemic model with latent period and nonlinear recovery rate. *Comput. Math. Methods Med.* **2018**, 7321694 (2018)
12. Liu, S., Ruan, S., Zhang, X.: Nonlinear dynamics of avian influenza epidemic models. *Math. Biosci.* **283**, 118–135 (2017)
13. Yang, X., Li, X.: Finite-time stability of linear non-autonomous systems with time-varying delays. *Adv. Differ. Equ.* **2018**, 101 (2018)
14. Hu, J., Sui, G., Lv, X., Li, X.: Fixed-time control of delayed neural networks with impulsive perturbations. *Nonlinear Anal., Model. Control* **23**(6), 904–920 (2018)
15. Yang, D., Li, X., Shen, J., Zhou, Z.: State-dependent switching control of delayed switched systems with stable and unstable modes. *Math. Methods Appl. Sci.* **41**(16), 6968–6983 (2018)
16. Li, X., Yang, X., Huang, T.: Persistence of delayed cooperative models: impulsive control method. *Appl. Math. Comput.* **342**, 130–146 (2019)
17. Ma, X., Wang, W.: A discrete model of avian influenza with seasonal reproduction and transmission. *J. Biol. Dyn.* **4**, 296–314 (2010)

18. Andronicoa, A., Courcoulb, A., Bronnerc, A., Scoizecd, A., Lebouquin-Leneveuet, S., Guinat, C., et al.: Highly pathogenic avian influenza H5N8 in South-West France 2016–2017: a modeling study of control strategies. *Epidemics* **28**, 100340 (2019)
19. Yang, X., Li, X., Xi, Q., Duan, P.: Review of stability and stabilization for impulsive delayed systems. *Math. Biosci. Eng.* **15**(6), 1495–1515 (2018)
20. Mu, R., Wei, A., Yang, Y.: Global dynamics and sliding motion in A(H7N9) epidemic models with limited resources and Filippov control. *J. Math. Anal. Appl.* **477**(2), 1296–1317 (2019)
21. Zhu, C., Li, X., Cao, J.: Finite-time H-infinity dynamic output feedback control for nonlinear impulsive switched systems. *Nonlinear Anal. Hybrid Syst.* **39**, 100975 (2021)
22. Xiao, Y., Xu, X., Tang, S.: Sliding mode control of outbreaks of emerging infectious diseases. *Bull. Math. Biol.* **74**, 2403–2422 (2012)
23. Zhou, W., Xiao, Y., Cheke, R.: A threshold policy to interrupt transmission of West Nile virus to birds. *Appl. Math. Model.* **40**(19–20), 8794–8809 (2016)
24. Bolzoni, L., Della Marca, R., Groppi, M.: Dynamics of a metapopulation epidemic model with localized culling. *Discrete Contin. Dyn. Syst., Ser. B* **25**(6), 2307–2330 (2020)
25. Chong, N., Smith, R.: Modelling avian influenza using Filippov systems to determine culling of infected birds and quarantine. *Nonlinear Anal., Real World Appl.* **24**, 196–218 (2015)
26. Li, W.X., Huang, L.H., Wang, J.F.: Dynamic analysis of discontinuous plant disease models with a non-smooth separation line. *Nonlinear Dyn.* **99**, 1675–1697 (2020)
27. Zhang, J., Jin, Z., Sun, G., Sun, X., Wang, Y., Huang, B.: Determination of original infection source of H7N9 avian influenza by dynamical model. *Sci. Rep.* **4**, 1–16 (2014)
28. Rappole, J.H., Hubalek, Z.: Migratory birds and West Nile virus. *J. Appl. Microbiol.* **94**, 475–585 (2003)
29. Filippov, A.: *Differential Equations with Discontinuous Righthand Sides*. Kluwer Academic, Dordrecht (1988)
30. Yang, Y., Zhang, T.: Modeling plant virus propagation with Filippov control. *Adv. Differ. Equ.* **2020**, 465 (2020)
31. Kuznetsov, Y.A., Rinaldi, S., Gagnani, A.: One parameter bifurcations in planar Filippov systems. *Int. J. Bifurc. Chaos* **13**, 2157–2188 (2003)
32. Li, X., Caraballo, T., Rakkiyappan, R., Han, X.: On the stability of impulsive functional differential equations with infinite delays. *Math. Methods Appl. Sci.* **38**(14), 3130–3140 (2015)
33. Li, X., Bohner, M.: An impulsive delay differential inequality and applications. *Comput. Math. Appl.* **64**(6), 1875–1881 (2012)
34. Utkin, V.I., Guldner, J., Shi, J.X.: *Sliding Mode Control in Electro-Mechanical System*, 2nd edn. Taylor & Francis, London (2009)
35. van den Driessche, P., Watmough, J.: Reproduction numbers and sub-threshold endemic equilibria for compartmental models of disease transmission. *Math. Biosci.* **180**, 29–48 (2002)
36. Leine, R.I.: *Bifurcations in Discontinuous Mechanical Systems of Filippov-Type*. The Universiteitsdrukkerij TU Eindhoven, The Netherlands (2000)
37. Leine, R.I., van Campen, D.H., van de Vrande, B.L.: Bifurcations in nonlinear discontinuous systems. *Nonlinear Dyn.* **23**, 105–164 (2000)
38. Chong, N., Dionne, B., Smith, R.: An avian-only Filippov model incorporating culling of both susceptible and infected birds in combating avian influenza. *J. Math. Biol.* **73**, 751–784 (2016)

Submit your manuscript to a SpringerOpen[®] journal and benefit from:

- Convenient online submission
- Rigorous peer review
- Open access: articles freely available online
- High visibility within the field
- Retaining the copyright to your article

Submit your next manuscript at ► [springeropen.com](https://www.springeropen.com)
